INFECTION AND IMMUNITY, Oct. 1993, p. 4415–4426
0019-9567/93/104415-12$02.00/0

Vol. 61, No. 10

# A Role for *Bacteroides fragilis* Neuraminidase in Bacterial Growth in Two Model Systems

VERONICA G. GODOY, MARY MILLER DALLAS, THOMAS A. RUSSO,† AND MICHAEL H. MALAMY*

*Department of Molecular Biology and Microbiology, Tufts University School of Medicine, 136 Harrison Avenue, Boston, Massachusetts 02111*

Received 6 May 1993/Returned for modification 3 June 1993/Accepted 30 July 1993

**Two *Bacteroides fragilis* neuraminidase-deficient mutants were used to study the role of neuraminidase activity in growth of *B. fragilis* in tissue culture monolayers (CHO cells) and in the in vivo rat granuloma pouch. The *nanH* structural gene for neuraminidase was cloned from *B. fragilis* TM4000 and was used to create two isogenic strains with chromosomal disruptions at the *nanH* gene. *B. fragilis* VRC404 contains an insertion flanked by disrupted copies of the *nanH* gene, and *B. fragilis* VRC426 contains a deletion of a significant portion of *nanH* coding sequences. The insertion mutant VRC404 is capable of reverting to *nanH*$^+$. It grew as well as the wild type in CHO monolayers. However, between 48 and 72 h after infection, the bacterial population was enriched with *nanH*$^+$ bacterial cells (10 to 20%). In the rat pouch 48 h after infection, more than 90% of the population sampled had become *nanH*$^+$. The deletion mutant VRC426 showed a severe growth defect in the rat pouch model. In addition, VRC426 was efficiently outgrown by the wild type in competition experiments, even when the mutant was present at 10 times the number of wild-type cells at the time of infection. A common characteristic of both model systems is a drastic decrease in the free glucose concentration 16 to 24 h postinfection. We suggest that neuraminidase activity may be required for *B. fragilis* to grow to maximal levels in the tissue culture and rat pouch systems by making other carbon sources available after glucose levels are reduced.**

*Bacteroides fragilis* is the most frequently isolated obligately anaerobic, non-spore-forming, gram-negative bacillus found in intra-abdominal and pelvic abscesses in humans (1). *B. fragilis* emerges as the prime anaerobic pathogen from the colonic flora, despite the fact that the organism is only a minority component of the normal anaerobic flora of the human gastrointestinal tract (1). Therefore, the organism must possess important virulence factors. To study these factors, we have begun to clone, mutagenize, and sequence genes that may play a role in the process of infection. With the cloned genes, we are creating isogenic *B. fragilis* mutants that differ from the wild type in only one trait.

One of the genes that could play a role in the infection process encodes the *B. fragilis* neuraminidase (24). The neuraminidases, or sialidases, are a group of glycohydrolase enzymes that cleave *N*-acetyl neuraminic acid (NANA [sialic acid]) residues from the termini of simple and complex oligosaccharides, glycolipids, gangliosides, and glycoproteins (9). Sialic acids are widely distributed on the surface of all eukaryotic cells (34). In the latter, the presence or absence of sialic acids on the surface of cells or tissues seems to be an important determinant of their physiological state. For example, neutrophils are removed from the circulation after desialylation. Also, desialylation results in the loss of function and clearance enhancement of immunoglobulins and certain components of the complement system (2, 14, 25, 29). This subject has been recently reviewed by Pilatte et al. (25).

It has been suggested that the presence of a neuraminidase activity may contribute to the virulence of several pathogenic bacteria (1, 5, 6, 11, 18, 20, 30, 39). However, as yet there is little evidence to establish an unequivocal role for neuraminidases in bacterial pathogenesis. Nevertheless, it has been recently reported (15) that the neuraminidase of *Vibrio cholerae* potentiates the activity of cholera toxin and, as a result, may contribute to the pathogenicity of this organism. In contrast, the neuraminidase of influenza A virus has a well-documented essential role for the attachment of the virus to host cells and for the prevention of attachment of additional virus particles to infected cells (8, 23, 36).

Many *B. fragilis* strains have neuraminidase activity, (3, 4, 37), and it has been suggested that this activity plays a role in the attachment of the bacteria to animal cells. However, this conclusion was based on indirect experiments in which *B. fragilis* was found to attach more efficiently to erythrocytes previously treated with the *V. cholerae* neuraminidase enzyme (16). We have described the cloning and partial sequencing of an *nanH* neuraminidase gene from *B. fragilis* clinical isolate TAL2480 (31). For this report, we constructed neuraminidase-deficient mutants of *B. fragilis* clinical isolate TM4000 and established a functional role for neuraminidase enzyme activity in growth of *B. fragilis* strains on tissue culture monolayers and in the rat granuloma pouches in vivo.

## MATERIALS AND METHODS

The bacterial strains and plasmids used in this work are described in Table 1.

**Growth of *B. fragilis* and *Escherichia coli* cells.** *B. fragilis*

* Corresponding author. Electronic mail address: In% "MMALAMY@Pearl.Tufts.Edu".

† Present address: Bacterial Pathogenesis Unit, Laboratory of Clinical Investigation, National Institute of Allergy and Infectious Diseases, Bethesda, MD 20892.

TABLE 1. Strains and plasmids used in the present work

| Strain or plasmid | Characteristics[a] | Source or reference |
|---|---|---|
| Strains | | |
| *E. coli* | | |
| DH5α | *F'/hsdR17 recA1 Δlaczya* (ϕ80*dlac ΔlacZ*M15) | 19 |
| DW1030 | *ΔlacX74 rpsE recA13* | 17, 28 |
| HB101 | *F⁻ Δ(mcrC-mrr) recA13 rpsL20* | 19 |
| *B. fragilis* | | |
| TC2 | NNMG-induced *nanH* mutant of TM4000 | 31 |
| JC101 | NNMG-induced arginine and histidine auxotroph of TM4000 | Laboratory strain |
| TM4000 | Wild-type *nanH*⁺, Rif^r | Laboratory strain |
| VRC404 | Insertional *nanH* mutant, Rif^r | This study |
| VRC426 | *nanH* defective by deletion | This study |
| Plasmids | | |
| Vectors and transfer factors | | |
| pUC7 | Amp^r *lacZα* | 19 |
| pUC12 | Amp^r *lacZα* | 19 |
| pJST61 | Cln^r, Amp^r *B. fragilis-E. coli* shuttle vector | 38 |
| pJST75 | Cef^r, Amp^r *B. fragilis-E. coli* shuttle vector | J. Thompson, this study |
| pJST55 | Cln^r, Amp^r *B. fragilis* suicide vector | 38 |
| pRK231 | RP4 derivative, Kan^r Tc^r Tra⁺ | 38 |
| *nanH*-containing plasmids | | |
| pTAR46 | 4.0-kb insert containing the *nanH* gene from TM4000 in pJST61 | This study |
| pVRC746 | 5.3-kb insert from pTAR46 containing the *nanH* gene from TM4000 in pUC7 | This study |
| pVRC463 | Derivative of pTAR46 with truncated *nanH* gene (downstream deletion) | This study |
| pVRC462 | Derivative of pTAR46 with truncated *nanH* gene (upstream deletion) | This study |
| pVRC4611 | 0.6-kb deletion of pTAR46 4.0-kb insert | This study |
| pVRC4602 | Internal *Bst*EII deletion of *nanH* in pTAR46 | This study |
| pVRC203 | *Hin*dIII fragment containing *nanH* gene cloned in pUC12 | This study |
| pVRC504 | 0.6-kb *nanH* internal fragment cloned into pJST55 | This study |
| pVRC5502 | *Bam*HI *nanH* deletion fragment from pVRC4602 cloned into pJST55 | This study |
| pVRC7511 | 1.5-kb *Eco*RI-*Bst*YI fragment from pTAR46 cloned into pJST75 | This study |

[a] Abbreviations: NNMG, *N*-methyl-*N'*-nitro-*N*-nitrosoguanidine; Amp, ampicillin; Rif, rifampin; Kan, kanamycin; Tc, tetracycline; Cln, clindamycin; Cef, cefoxitin; Tra⁺, transfer proficient.

cells were routinely grown on BHIS medium (Difco, Detroit, Mich.) broth or agar plates supplemented with 5 μg of hemin (Sigma Chemical Co., St. Louis, Mo.) per ml. *B. fragilis* cells were incubated in a Coy anaerobic chamber (Ann Arbor, Mich.) containing a gas mixture of 5% $CO_2$, 10% $H_2$, and 85% $N_2$ at 37°C. The BHIS medium was supplemented with the following antibiotics (obtained from Sigma Chemical Co. unless otherwise noted) as required: clindamycin (6 μg/ml [Upjohn Co., Kalamazoo, Mich.]), streptomycin (200 μg/ml), gentamicin (50 μg/ml), cefoxitin (25 μg/ml [Merck, Sharpe & Dohme, West Point, Pa.]). SAMM agar, a variation of AMM minimal broth (38), containing 0.02% hemin was used as the plating medium to differentiate the *B. fragilis* wild type from auxotrophs. *E. coli* cells were grown routinely in L medium (19) broth or plates with ampicillin (200 μg/ml), spectinomycin (40 μg/ml), or tetracycline (20 μg/ml) when appropriate.

**Recombinant DNA techniques.** All recombinant DNA techniques were performed as described by Maniatis et al. (19). The restriction enzymes were obtained from New England Biolabs (Beverly, Mass.) and were used as suggested by the manufacturer.

**Cloning the *nanH* gene from *B. fragilis* TM4000.** TM4000 chromosomal DNA was digested to completion with the restriction enzymes *Bgl*II and *Bam*HI. In a preliminary experiment, we determined by Southern hybridization analysis that these enzymes create a single band approximately 7 kb in size that shows homology when TM4000 chromosomal DNA is probed with DNA containing the *nanH* gene from TAL2480. Therefore, *B. fragilis* TM4000 chromosomal fragments between 4 and 10 kb in size were purified from a low-melting-point agarose gel (0.7%; FMC Bioproducts, Rockland, Maine) and cloned into the *Bgl*II site of shuttle vector pJST61 (31) to construct a library of the TM4000 chromosome in *E. coli* HB101. To detect the clone containing the *nanH* gene, the library was plated onto L ampicillin plates, at about 200 colonies per plate, transferred to membranes, and hybridized to the DNA probe containing the *nanH* gene from TAL2480. One positive clone containing an approximately 6-kb insert was detected among 720 colonies screened and found to possess neuraminidase activity. A partial *Bst*YI digest of the 6-kb insert was ligated to pJST61. Neuraminidase-positive clones that contained a plasmid with a 4.0-kb insert were found. The *nanH* gene in the 4.0-kb fragment present in pTAR46 was localized by subcloning experiments (Fig. 1).

**Construction of neuraminidase-deficient mutants.** The insertion mutant VRC404 was constructed by cloning a 2.0-kb *Hin*dIII fragment from pVRC746 into the *Hin*dIII site of pUC12, giving rise to pVRC203 (Fig. 2). A 0.7-kb *Bst*YI-*Bam*HI fragment, internal to *nanH*, was isolated from pVRC203. This fragment was cloned into pJST55, creating pVRC504. This final plasmid was delivered into *B. fragilis* TM4000 by conjugation as described below.

Mutant VRC426, was created by purifying a 3.0-kb *Bst*YI fragment from pVRC4602 and cloning it into the *Bgl*II site of

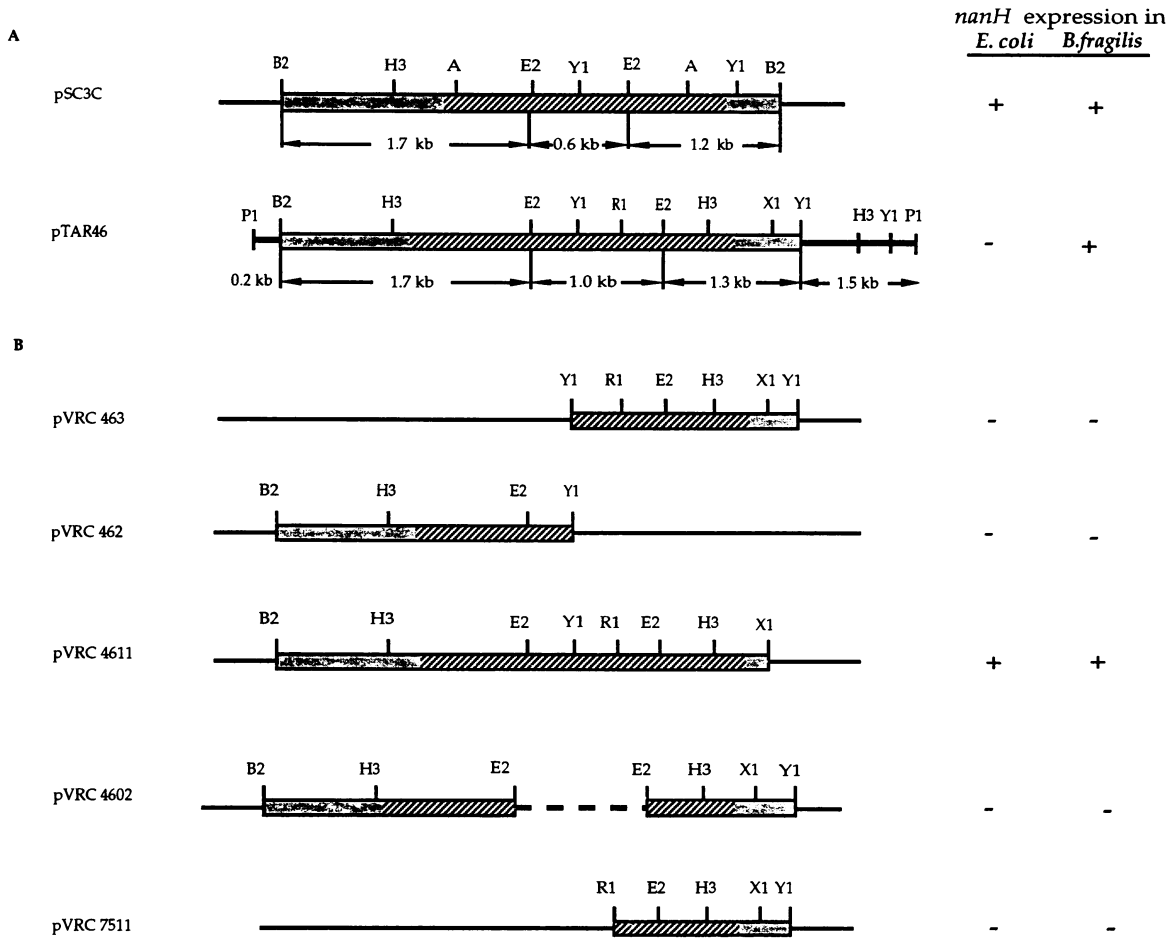


FIG. 1. (A) Partial restriction maps of plasmids pSC3C and pTAR46, which carry the cloned *nanH* genes from TAL2480 and TM4000, respectively. Thick lines represent the vector backbone (pJST61). The hatched areas within the cloned inserts show the approximate localization of the *nanH* gene. The neuraminidase expression of these clones in *B. fragilis* and *E. coli* is shown to the right of the figure. Whether or not neuraminidase expression is observed in *E. coli* or *B. fragilis* is denoted by a + or a −, respectively. (B) Subcloning of pTAR46. The restriction maps of the subclones are drawn with respect to pTAR46. The neuraminidase expression of the different subclones is shown to the right of each subclone. The details of the subcloning of pTAR46 are as follows. The plasmid pVRC746 contains a 5.7-kb (1.7 kb is from pJST61 [see panel A]) *Pst*I fragment from pTAR46 cloned into pUC7. Subclone pVRC463 was constructed by cloning a 1.8-kb *Bst*YI fragment from pTAR46 into pJST61. pVRC462 contains a 2.2-kb *Bst*YI fragment from pTAR46 cloned into the *Bgl*II site of pJST61. The same two *Bst*YI fragments were also cloned into the *Bam*HI site of pUC7, giving rise to pVRC763 and pVRC762, respectively. pVRC4610, a pUC7 intermediate, was made by dropping out a 2.1-kb *Xho*I-*Sal*I fragment (which includes 0.6 kb of the 4.0-kb insert) from pVRC746. This plasmid was treated with *Bam*HI, and a 3.6-kb *Bam*HI fragment was isolated and cloned into the *Bgl*II site of pJST61 to create pVRC4611. pVRC4602 was made by deleting a 0.9- to 1.0-kb *Bst*EII fragment from pVRC746. A 4.7-kb *Bam*HI fragment from this intermediate plasmid (pVRC4601) was then cloned into the *Bgl*II site of pJST61. The pVRC7263 intermediate was made by cloning a 1.6-kb *Eco*RI-*Bam*HI fragment from pVRC763 into the multiple cloning site of pSP72 (Promega, Madison, Wis.). A 1.6-kb *Bgl*II-*Bam*HI fragment was cloned into the *Bgl*II site of pJST75 to create pVRC7511. Abbreviations: A, *Ava*I; B2, *Bgl*II; E2, *Bst*EII; Y1, *Bst*YI; R1, *Eco*RI; H3, *Hin*dIII; P1, *Pst*I; X1, *Xho*I.

pJST55. The resulting plasmid, pVRC5502, was also delivered into *B. fragilis* TM4000 by conjugation (see Fig. 4).

**Colony filter hybridization.** The colony filter hybridization method used is described by Maniatis et al. (19). The 3.5-kb *Bgl*II fragment containing the whole *nanH* gene from TAL2480 (31) was used as a probe. This probe was radioactively labelled with [$\alpha$-$^{32}$P]dCTP obtained from NEN Research Products (Boston, Mass.) by random oligonucleotide priming (19).

**DNA hybridization analysis.** DNA hybridization analysis was performed by the method of Southern (35). Approximately 10 $\mu$g of chromosomal DNA was digested to completion with the appropriate restriction enzyme(s), typically in a 100-$\mu$l reaction mixture. The DNA digest (2.5 $\mu$g) was subjected to electrophoresis in a 1% agarose gel (FMC Bioproducts) and transferred by capillarity to a nylon membrane (Boehringer Mannheim Biochemica, Mannheim, Germany) according to the alkaline method (27). DNA fragments were fixed to the membrane by baking the membrane at 80°C for 30 min. Hybridization probes were prepared by purifying the appropriate restriction fragments from agarose gels with the GeneClean kit (Bio 101, Inc., La Jolla, Calif.) and then labeling the fragments with digoxigenin-dUTP by random-primed DNA synthesis as described in the instructions to the Genius kit (Boehringer Mannheim Biochemica). All steps were performed in siliconized glass tubes which were incubated in a hybridization incubator at 65°C (model 310; Robbins Scientific Corporation, Sunnyvale, Calif.).

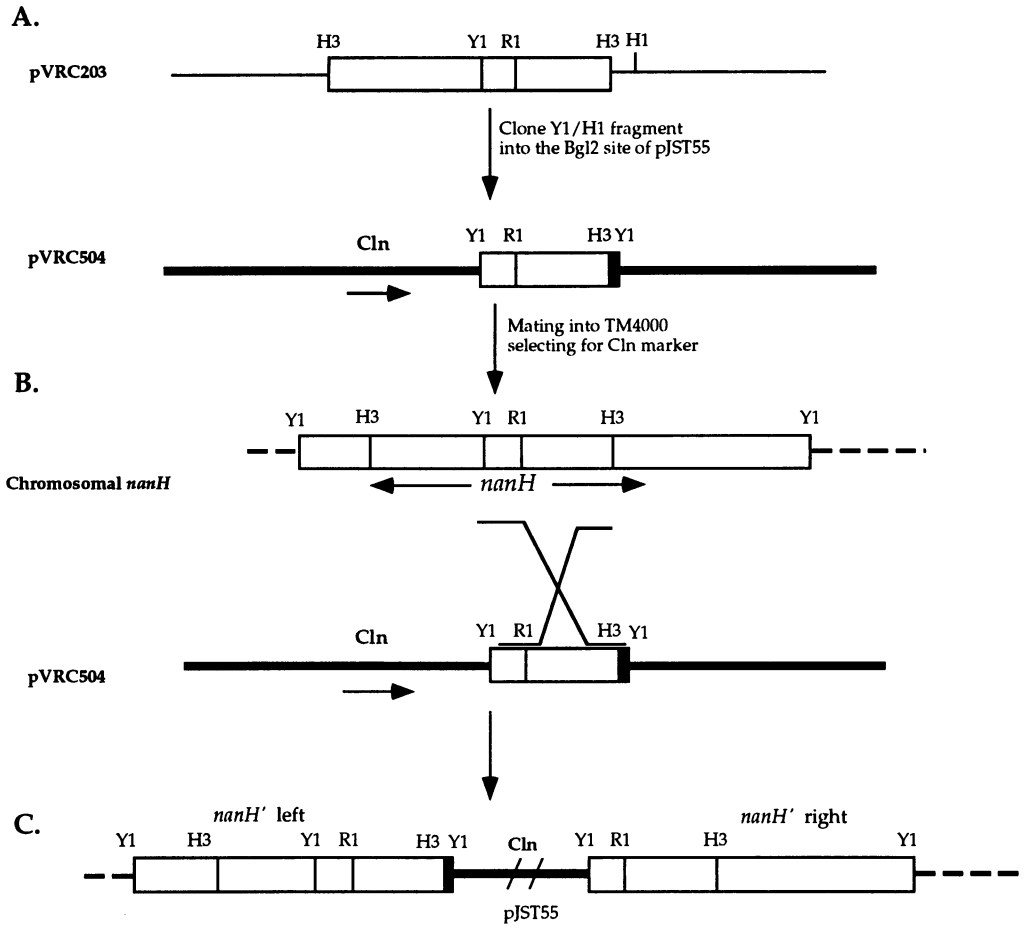


FIG. 2. Construction of *B. fragilis* VRC404. (A) Starting plasmids. The restriction maps of the starting plasmid pVRC203 and the intermediate plasmid pVRC504 are shown. Plasmid pVRC203 is shown containing the *nanH* fragment in the appropriate orientation to isolate the 0.7-kb *Bst*YI-*Hin*dI internal fragment (for a restriction map of *nanH*, see Fig. 1). The rectangles represent internal *nanH* sequences, the thin lines represent DNA from pUC12, and the thick black lines DNA from pJST55. The small black rectangle in pVRC504 indicates the linker region taken from pUC12. The details of the plasmid constructions are given in Materials and Methods. (B) Diagram of homologous recombination between pVRC504 and the *B. fragilis* chromosome at the *nanH* locus to form the cointegrate VRC404. The insertional inactivation of the *nanH* gene by pJST55 is drawn as a thick black line flanked by the right and left portions of the *nanH* gene. The creation of a new *Bst*YI fragment in *nanH'* left is shown as well. The dashed black lines represent the rest of the TM4000 chromosome. H1, *Bam*HI; the other restriction enzyme abbreviations are defined in the legend to Fig. 1. Cln, clindamycin resistance gene. The maps are not to scale.

After incubation, the filters were treated with the chemiluminescent substrate for alkaline phosphatase, Lumi-Phos 530 (Boehringer Mannheim Biochemica), and exposed to Kodak XAR-5 X-ray film for 2 to 30 min.

**DNA transfer from *E. coli* to *B. fragilis*.** Chimeric plasmids were mobilized into *B. fragilis* by bacterial conjugation as previously described (31). *B. fragilis* transconjugants were selected on BHIS plates supplemented with streptomycin, clindamycin, and gentamicin. Selected transconjugants were purified on the same media.

**Growth of *B. fragilis* on tissue culture monolayers.** These experiments were based on the protocols of Claesson and Gotthardsson (7). Chinese hamster ovary (CHO; pro5) cells were originally obtained from Ralph Isberg, Tufts University School of Medicine, and were routinely grown in RPMI 1640 medium (Sigma Chemical Co.) supplemented with 10% fetal bovine serum (Hyclone Lab. Inc., Logan, Utah), 2 mM L-glutamine (Sigma Chemical Co.) and 10 μg of gentamicin (GIBCO BRL Life Technologies Inc., Grand Island, N.Y.) per ml. T25 tissue culture flasks (Corning Laboratory Sciences Co., Corning, N.Y.) were seeded at $5 \times 10^4$ cells per ml and incubated at 37°C in a 5% $CO_2$ incubator. Under these conditions, the tissue culture monolayers reached confluency ($10^6$ cells per ml) after 36 h of incubation. Just prior to infection, the spent growth medium was removed and 8 ml of fresh prewarmed medium was added to the flasks. The confluent monolayers were infected with anaerobically grown *B. fragilis* cells diluted in buffered saline and added to achieve a final concentration of approximately $5 \times 10^6$ CFU per flask. The infected flasks were placed in a tissue culture incubator in normal air supplemented with 5% $CO_2$. The *B. fragilis* cell titer at time zero was determined for every infected flask immediately after inoculation by taking a 0.1-ml sample from the tissue culture medium. Bacterial growth was measured by determining viable counts at several time points after the CHO monolayers were infected.

The culture medium was removed and sampled for viable bacteria. The tissue culture monolayers were resuspended in 5 ml of buffered saline, and the viable bacterial cell titer was determined. The total bacterial cell titers reported for the tissue culture experiments are the sum of the fractions described above.

**Growth of *B. fragilis* in the rat granuloma pouch.** Rat granuloma pouches were formed in Wistar male rats essentially as described by Dalhoff et al. (12). A mixture of croton oil and corn oil (instead of olive oil) was used to initiate the inflammatory response. The resulting sterile granuloma pouches were infected with *B. fragilis* cells at different inoculum sizes ($10^3$ to $10^7$ bacteria per ml) by injecting 1 ml of appropriate dilutions of the bacterial cells into the pouches. Bacterial titers in the pouches were determined throughout the experiment by removing approximately 0.2 ml of pouch fluid with a tuberculin syringe (1 ml) with a 27-gauge needle and plating suitable dilutions on BHIS media. The initial inoculum size within the pouch at time zero was experimentally determined in all cases unless otherwise specified. Generally, the rat granuloma pouch was sampled for 1 week after infection.

**Enzyme assays.** The neuraminidase assay was performed as described by Myers et al. (21). The bacterial cell extracts used for the enzyme assays were prepared by sonication. The *B. fragilis* cells used in these experiments were grown in defined medium supplemented with either glucose (0.5%) or NANA (0.5%; Sigma Chemical Co.).

**Determination of glucose concentrations in the rat pouch fluid and in the supernatant of CHO cells.** Samples were obtained and immediately centrifuged at low speed in an Eppendorf 5415C microcentrifuge (Brinkmann Instruments Co., Westbury, N.Y.) to remove the particulate material, i.e., cell debris, bacterial cells, and erythrocytes. The supernatant was collected and used for glucose determination. The glucose oxidase assay was carried out according to the indications of the supplier (Sigma Chemical Co.).

**Sample preparation for scanning electron microscopy.** CHO cells were seeded onto 13-mm coverslips (Thermanox; Miles Scientific, Naperville, Ill.) in a six-well dish (Costar Co., Cambridge, Mass.) and allowed to reach confluency. Each of the six wells was infected with $6 \times 10^5$ *B. fragilis* cells. Bacterial cells and CHO cells were fixed onto the coverslips at 24, 48, and 65 h after infection; the wells were washed twice with buffered saline, 3 ml of phosphate-buffered saline and 1.5 ml of an 8% glutaraldehyde solution were added, and the dishes were kept on ice for 1 h. The glutaraldehyde solution was removed by aspiration, and 4 ml of 0.1 M phosphate buffer (pH 7.5) was added. This buffer was removed after 10 min and replaced with 6 ml of 70% ethanol. The dishes were kept at 4°C until they were processed for electron microscopy. Scanning electron microscopy was done with an ISI-DS-130 scanning electron microscope according to standard procedures (26).

## RESULTS

**Cloning of the *nanH* gene from TM4000.** In order to construct isogenic *nanH*-deficient mutants of *B. fragilis* TM4000, we first cloned the *nanH* gene from TM4000 into vector pJST61. The correct clones were detected on the basis of their homology to the *nanH* gene from *B. fragilis* TAL2480 (31). The procedures for cloning and subcloning the *nanH* gene are given in Materials and Methods. Three independent neuraminidase-producing transformants were detected in *E. coli* HB101; the three candidates contained identical DNA inserts approximately 4.0 kb in size. One of these plasmids was used for further analysis and was named pTAR46 (Fig. 1). pTAR46 was transferred by conjugation to *nanH*-deficient *B. fragilis* TC2 (31) (see Materials and Methods) and expressed high levels of neuraminidase activity when grown in SAMM broth supplemented with 0.5% NANA (data not shown).

**Analysis of the *nanH* gene in pTAR46.** A restriction map of the insert in pTAR46 was constructed with several enzymes. Comparison of the restriction map (Fig. 1) of the *nanH* region of TM4000 cloned in pTAR46 with that of TAL2480 contained in pSC3C (31) reveals some similarities, but the two *nanH* genes are not identical.

The location of the *nanH* gene within the 4.0-kb insert is based on a restriction mapping comparison with the *nanH* gene from TAL2480 carried in plasmid pSC3C and the neuraminidase activities of pTAR46 and derivatives. First, *B. fragilis* or *E. coli* strains carrying pVRC463 and pVRC462 (Fig. 1), each with a *Bst*YI insert approximately half the size of pTAR46, do not express neuraminidase activity. Therefore, as is the case for pSC3C, we conclude that the *Bst*Y1 site is within the *nanH* gene. Second, plasmid pVRC4611 contains a deletion of all of the DNA present in the 4.0-kb fragment to the right of the *Xho*I site. This plasmid expresses neuraminidase activity in both *B. fragilis* and *E. coli*. However, expression of neuraminidase activity from pVRC4611 in *B. fragilis* is different from that of pTAR46; the neuraminidase activity of this clone is higher than the wild type when it is grown in media without free NANA. This suggests that there may be regulatory sites in the region between the *Xho*I site and the rightmost *Bst*Y1 site. Therefore, the coding region of the *nanH* gene must be to the left of the *Xho*I site. Third, the lack of neuraminidase activity in strains containing pVRC4602, a *Bst*EII deletion of pTAR46, indicates that the *Bst*EII fragment must include *nanH* sequences. Finally, pVRC7511-containing strains which carry an even larger deletion do not synthesize neuraminidase activity, in agreement with the result for strains carrying pVRC4602. Taking all of these results together, we can localize the *nanH* gene to a region between the *Xho*I site and the leftmost *Hin*dIII site (Fig. 1). These results are in agreement with preliminary sequence data (unpublished results) on this DNA and with the protein sequence of a *B. fragilis* neuraminidase reported by Tanaka et al. (37).

**Isolation of chromosomal insertion and deletion mutations in the *nanH* gene of TM4000.** Two independent mutations of the chromosomal *nanH* gene of *B. fragilis* TM4000 were constructed: (i) insertion of a plasmid into the coding region of the gene and (ii) deletion of a portion of the structural gene.

To construct the insertion mutation, we took advantage of homologous recombination between the chromosomal *nanH* gene and pVRC504, which contains an internal fragment of the *nanH* gene incorporated into the suicide plasmid pJST55 (38). The resulting strain, VRC404, contains pJST55 integrated into the chromosome flanked by two disrupted copies of the *nanH* gene. The construction steps are diagrammed in Fig. 2 and are explained in detail in Materials and Methods. In order to deliver pVRC504 (Fig. 2A) into the *B. fragilis* chromosome, an *E. coli* donor strain containing pVRC504 and the mobilizing plasmid pRK231 was mated with *B. fragilis* TM4000, followed by isolation of $Cln^r$ *B. fragilis* derivatives. We obtained 10 $Cln^r$ colonies from four independent matings, and each isolate was found to be defective in neuraminidase activity. To confirm the structure of the

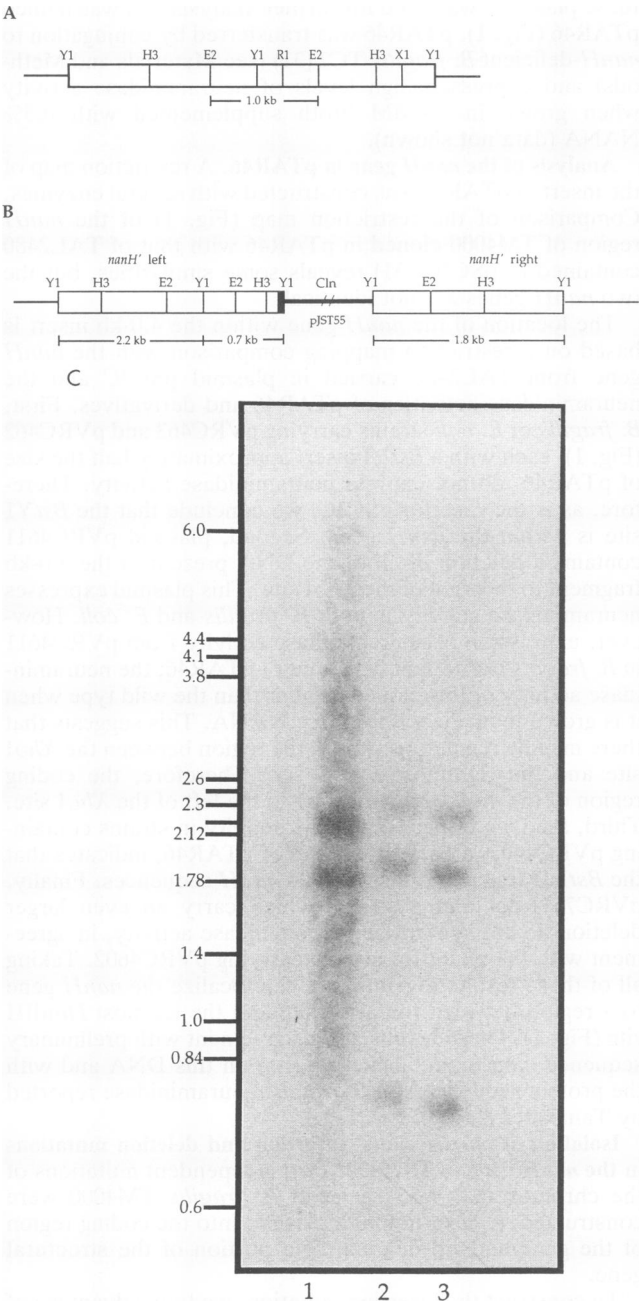


FIG. 3. Proof of the structure of VRC404 by Southern blot hybridization. (A) Source of the probe. The DNA probe used is indicated by the size bar underneath the restriction map of pTAR46 (top diagram). The details of this experiment are in Materials and Methods. (B) Schematic of the *nanH* region in VRC404. All DNAs were restricted to completion with *Bst*YI. The pertinent restriction sites are shown. The sizing bars indicate the expected sizes of the DNA fragments generated by *Bst*YI restriction that should be detected by the DNA probe shown in panel A. (C) Luminogram of the DNA hybridization. The size standard, a T7 *Hpa*I DNA ladder, is shown to the left. Lanes: 1, pTAR46 plasmid; 2, VRC403; 3 VRC404 chromosomal digests. The restriction site abbreviations are defined in the legend to Fig. 1.

insertion derivatives, chromosomal DNA was prepared from each of the candidates and analyzed by Southern hybridization as shown in Fig. 3. A 1.0-kb *Bst*EII fragment isolated from pTAR46 was used as the probe (Fig. 3A). The expected 2.2- and 1.8-kb fragments (Fig. 3B) are seen in the control sample (Fig. 3C, lane 1) and in the chromosomal DNA from the Cln$^r$ candidates (lanes 2 and 3), respectively. The DNA from candidate strains VRC403 and VRC404 (lanes 2 and 3) shows an additional 0.7-kb fragment that results from the duplication of a segment of *nanH* DNA during the recombination reaction that integrated the suicide plasmid into the chromosome (Fig. 2). All of the independent candidates showed this extra DNA band. Strain VRC404 was chosen for further study.

A second mutant (VRC426) that contains a deletion of part of the *nanH* coding sequence was isolated from a cointegrate intermediate formed by recombination between the wild-type *nanH* gene on the chromosome and a *nanH* gene with an internal deletion carried on pJST55. The series of reactions to create VRC426 are presented in Fig. 4 (for details on plasmid constructions, see Materials and Methods). An *E. coli* donor strain containing pVRC5502 and pRK231 was mated with *B. fragilis* TM4000, and Cln$^r$ transconjugants were isolated. Because the resulting cointegrate (VRC122 [Fig. 4B]) contains an intact *nanH* gene as well as the gene with the internal *Bst*EII deletion, neuraminidase activity could be detected in extracts prepared from all candidates. Resolution of the cointegrate intermediate by homologous recombination could generate two different *nanH* products (Fig. 4B and C): a wild-type *nanH* gene or a *nanH* gene with a *Bst*EII deletion. To detect resolution products of the cointegrates, we screened for Cln$^s$ strains by a replica plating technique. Eleven Cln$^s$ colonies were isolated after screening approximately 35,000 colonies. Six of the 11 Cln$^s$ strains had become neuraminidase deficient.

To verify the structure of the Cln$^s$ *nanH*-deficient candidates, Southern hybridization analysis was performed on their chromosomal DNA, DNA from the parental cointegrates, and the starting strain TM4000. Figure 5C shows the results of probing *Bst*YI chromosomal digests of these DNAs with the 4.7-kb *Pst*I fragment from pVRC4602, the *Bst*EII deletion of pTAR46. The details of the probe used and the expected restriction products are also shown in Fig. 5 (panels A and B). Lane 1 shows the products of cointegrate VRC122. The 1.8- and 2.2-kb bands demonstrate the presence of the wild-type copy of the *nanH* gene. These bands are also present in lane 2, which contains the digest of the wild-type chromosomal DNA. Lane 1 also shows a 3.0-kb band which represents the deleted version of the *nanH* gene present in the cointegrate. The small band about 0.9 kb in size in lane 1 is part of the vector which is contained in the probe (Fig. 5A), confirming that the pJST55 suicide vector is also present in the cointegrate intermediate. VRC426, the neuraminidase-deficient strain shown in lane 3, contains only the 3.0-kb *Bst*YI fragment corresponding to the *nanH* gene with the internal *Bst*EII deletion.

**Properties of VRC404 and VRC426.** The in vitro growth of the neuraminidase-deficient strains on standard laboratory media such as BHIS and SAMM supplemented with glucose was unaffected by insertion or deletion mutations (data not shown). *B. fragilis* replicons showed the same stability in these strains compared with the wild type, and no alterations in the ability to serve as recipients of conjugal elements was observed. VRC404 gave rise to neuraminidase-positive re-

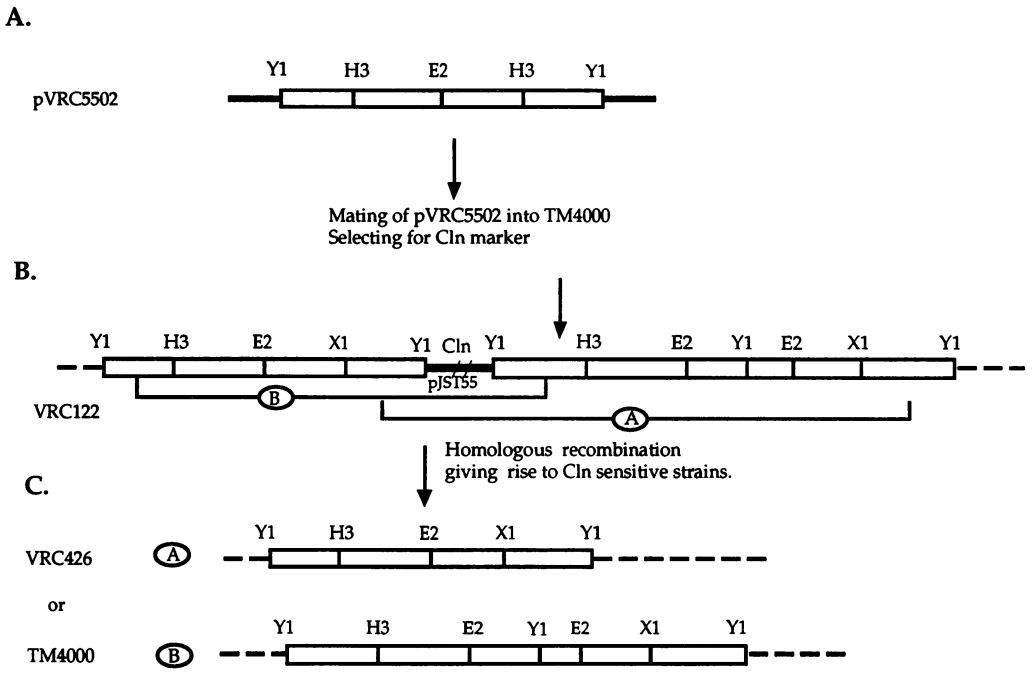


FIG. 4. Construction of the *nanH* deletion mutant VRC426. (A) Starting plasmid. The cloned fragment in pVRC5502 is the same as in pVRC4602 (Fig. 1), but the backbone is now pJST55. pVRC5502 and the TM4000 chromosome can recombine at the *nanH* locus, generating the cointegrate intermediate depicted in panel B. (B) Diagram of the TM4000 chromosome at the recombination site in VRC122, the cointegrate intermediate. The restriction mapping is the same as described above. The two possible products resulting from homologous recombination within this cointegrate are indicated by the brackets underneath the map of VRC122. (C) Resolution products. The resolution of the cointegrate gives rise to $Cln^s$ strains that will be either wild type (B) or mutant (A) for neuraminidase. The maps are not to scale, and only relevant restriction sites are shown. The restriction site abbreviations are defined in the legend to Fig. 1.

vertants at a frequency of $10^{-3}$ to $10^{-4}$. VRC426 did not give rise to neuraminidase-expressing revertants under the same conditions.

**Growth of *B. fragilis* TM4000 and the *nanH*-deficient strains on tissue culture monolayers.** *B. fragilis* strains can grow on tissue culture monolayers incubated in air supplemented with 5% $CO_2$ (7). However, as reported by Claesson and Gotthardsson (7), studying the growth of *B. fragilis* on mouse embryo fibroblasts, the *B. fragilis* cells begin to grow only when an appropriate partial $O_2$ pressure ($pO_2$) and redox potential are established. This requires active interaction of the bacterial and the animal cells. They reported that 16 h after the addition of fresh media with or without bacteria, the monolayers had reached a $pO_2$ and a redox potential low enough to allow the survival of *B. fragilis* but not growth. After this time, in the infected monolayers only, the *B. fragilis*-tissue culture cell interactions result in a lowering of the $pO_2$ and redox potential to the level necessary for bacterial growth (7). Although it has been determined that an intact actively metabolizing monolayer is an absolute requirement for *B. fragilis* growth in this system, exactly how the *B. fragilis* cells grow under these conditions is not known. To begin to address this question, scanning electron microscopy was used to monitor the growth of wild-type *B. fragilis* TM4000 on CHO cell monolayers (Fig. 6). At early times after infection (24 h [panel B]), isolated bacterial cells can be seen on the surface of the CHO cells. Most of the tissue culture cell surface is free of bacteria. At 48 h (panel C), a larger number of bacterial foci containing between three and five bacterial cells are observed on the surface of the tissue culture cells. At later times (65 h [panel D]), large clusters of bacteria in microcolonies (of approximately ≥100 cells) are prominent on the surface of the CHO cells. However, even at this time, large portions of the tissue culture cell surface are free of bacteria. Consequently, these experiments show that when *B. fragilis* grows it covers only a portion of the animal cell surface.

A quantitative growth curve of *B. fragilis* TM4000 on CHO cell monolayers is shown in Fig. 7. We determined that TM4000 started to grow under these conditions only after 16 h postinfection (data not shown) and reached a final cell titer of $3 \times 10^9$/ml after 48 h of incubation. Growth of VRC404, the *nanH* insertion mutant, on the tissue culture monolayers was similar to that of TM4000 (data not shown). However, at late times after infection (30 to 40 h), approximately 20% of the VRC404 colonies tested by replica plating had become $Cln^s$ and neuraminidase positive. For VRC404 to become $Cln^s$, there must be a recombination event involving the *nanH* homologous flanking regions that were generated as a result of the insertional recombination of pJST504 into the chromosome (Fig. 2C). This recombination event occurs at low frequency ($10^{-3}$ to $10^{-4}$) in in vitro-grown cultures of VRC404. The enrichment for revertants during growth of VRC404 on tissue culture cells suggests that there is strong selective pressure for $nanH^+$ cells in the tissue culture system. This may occur if neuraminidase activity becomes important to obtain nutrients for bacterial cell growth. Indeed, we found that the glucose concentration in the infected tissue culture flasks during active bacterial growth decreased from 11 to 14 mM (approximately 0.2%) at time zero to 2.9 mM at 14 h, and no detectable free glucose was found after 22 h postinfection. The glucose concentration was also low (3.2 mM) in an uninfected CHO monolayer at 16 h. These results establish that 14 h after infection, the infected sys-

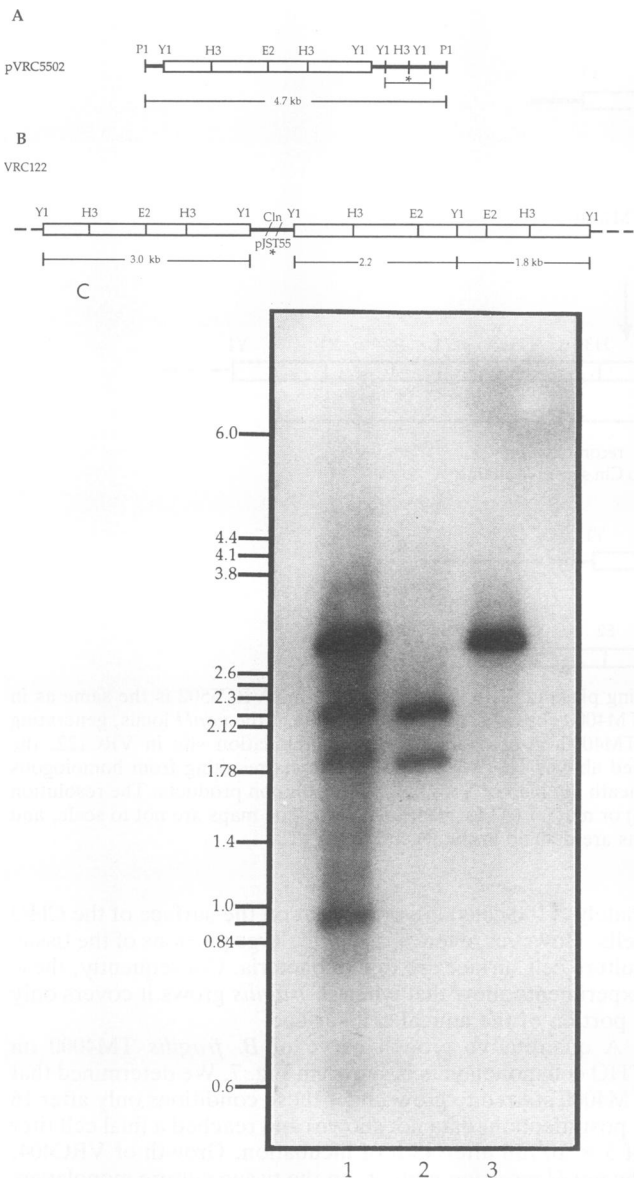


FIG. 5. Proof of the structure of VRC426 by Southern hybridization. (A) Source of the probe. The DNA probe used is indicated by the sizing bar underneath the restriction map of pVRC5502. The thick lines represent pJST55 backbone. (B) Schematic of the chromosomal cointegrate. The cointegrate contains all of the possible *Bst*YI DNA fragments that should hybridize to the DNA probe drawn in panel A. The sizes of these restriction fragments are shown underneath the map. All of the map indications are the same as in Fig. 2. The maps are not to scale. The details are explained in Materials and Methods and in the text. The asterisk underneath pJST55 indicates that the 0.9-kb *Bst*YI fragment present in VRC122 comes from the vector. (C) Luminogram of the DNA hybridization. The size standard, a T7 *Hpa*I DNA ladder, is shown at the left. Lanes: 1, VRC122; 2, TM4000; 3, VRC426. All of the samples are chromosomal DNA restricted to completion with *Bst*YI. The restriction site abbreviations are defined in the legend to Fig. 1.

tem, consisting of tissue culture cells and bacteria, is under glucose limitation. When adequate glucose concentrations are maintained throughout the *B. fragilis* growth phase by periodic addition of glucose to the medium to a concentration of 28 mM, the reversion of VRC404 to *nanH*$^+$ was not observed.

We also examined the growth properties of *B. fragilis* VRC426, the *nanH* deletion strain, in the CHO monolayer system (Fig. 7). While the increase in VRC426 cells was slower than that of wild-type TM4000 during the first 24 h of incubation, the final bacterial yield at 70 h was similar. The lag phase before VRC426 began to grow was 2 to 4 h longer than that for the wild-type strain (data not shown). This initial growth deficiency of VRC426 could be restored by supplying the *nanH* gene in *trans* on pTAR46 (Fig. 7) while the addition of the parental cloning vector (pJST61) to VRC426 did not alter the growth defect. In addition, pTAR46 is retained in 100% of the VRC426 cells recovered from the tissue culture system while the pJST61 parental vector was rapidly lost under the same growth conditions. It is known that pJST61 and its derivatives are unstable in *B. fragilis* in the absence of selective pressure (clindamycin) in vitro. Therefore, the retention of pTAR46 by the mutant VRC426 is an indication that the information present in this plasmid is important for the growth of the bacterial cells and suggests that the growth conditions of the tissue culture monolayers create the selective pressure for plasmid retention.

The results obtained with the tissue culture system and the wild-type or *nanH*-deficient *B. fragilis* strains suggest that neuraminidase activity is important but not essential for the growth of *B. fragilis* in this system.

**Growth of *B. fragilis* TM4000 and the *nanH*-deficient mutants in the rat granuloma pouch.** The *nanH*-deficient mutants were also tested in a true in vivo model system, the rat granuloma pouch.

When *B. fragilis* VRC404, containing the *nanH* insertion mutant, was used to infect the granuloma pouch, a growth curve similar to that obtained with the wild-type strain TM4000 was observed. However, just as in the tissue culture system, *nanH*$^+$ revertants were isolated among the progeny cells. In this case, however, revertants were detected at 24 h postinfection (about 5% of the colonies isolated), and by 48 h after infection more than 90% of the bacteria were *nanH*$^+$ (Fig. 8A). Therefore, it appears that strong selective pressure for the emergence of *nanH*$^+$ cells is also present in the granuloma pouch. As in the tissue culture system, we found that the glucose concentration in the rat pouch fluid fell to low levels (1 mM) 24 h after *B. fragilis* infection.

In contrast to the results obtained in the tissue culture system, the nonreverting *nanH* deletion strain VRC426 grew more slowly and reached a lower plateau level in the rat pouch than the wild type (Fig. 8B). In this system, we also observed a lag time of approximately 16 h before bacterial growth began for all the strains tested. This suggests that, as in the tissue culture system, this time period reflects the host and bacterial activities required to attain the appropriate $pO_2$ and redox potentials for *B. fragilis* growth. The dip observed in the growth curve of the *B. fragilis* strains at initial times after infection occurred in all of the experiments, although the magnitude of the dip varied. The significance of this dip is not clear.

In competition experiments in which *nanH*$^+$ cells (JC101) and VRC426 cells were mixed at the time of infection, the wild-type cells quickly outgrew the mutant cells even when the initial ratio of mutant cells to wild-type cells was 10-fold greater (Fig. 8C).

**Complementation of the VRC426 growth defect in the rat pouch.** The inability of VRC426 to grow in the rat pouch system could be reversed by the addition of the *nanH*$^+$-

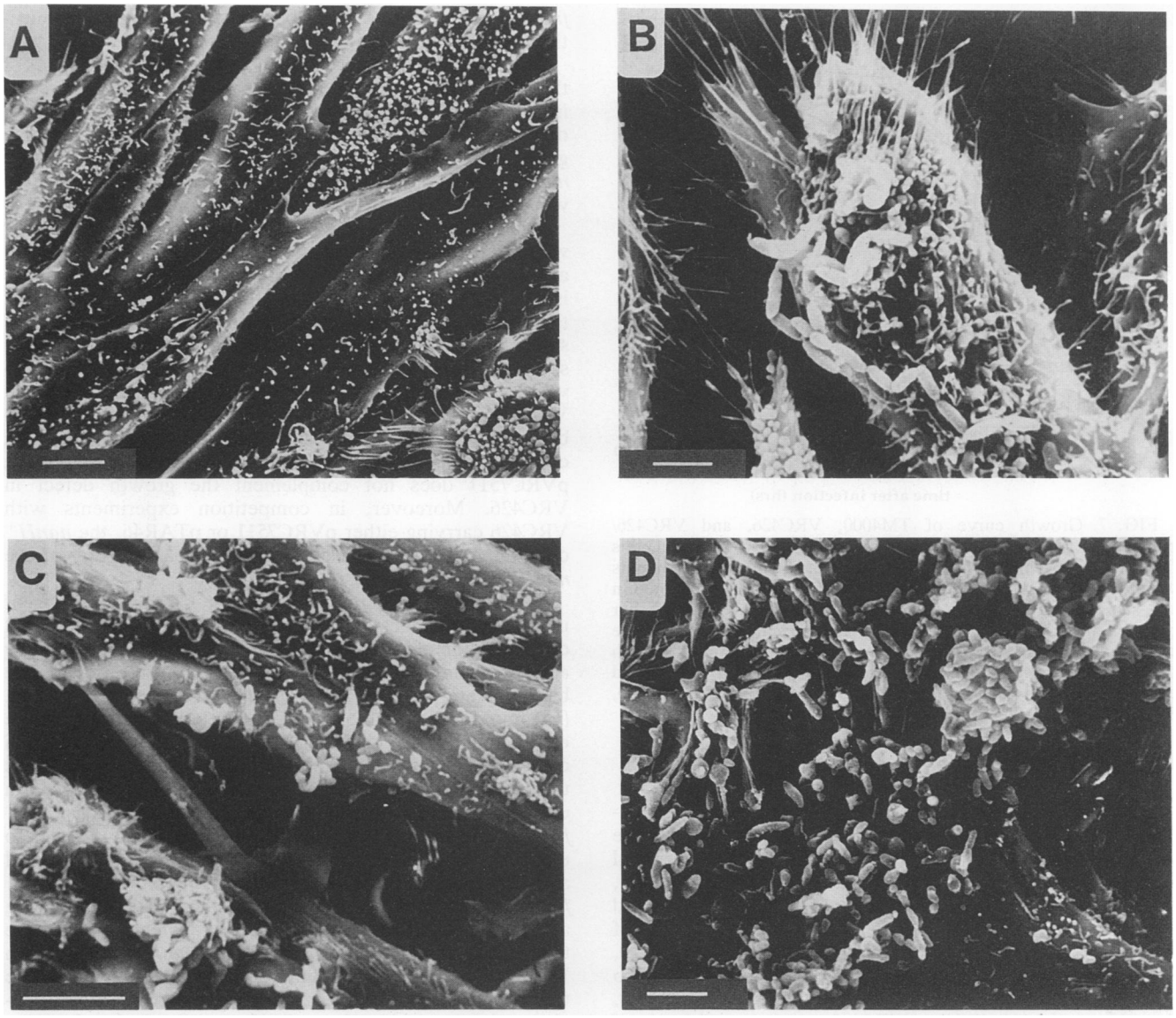


FIG. 6. Scanning electron micrographs of CHO monolayers at different times after infection with *B. fragilis* TM4000. (A) Uninfected CHO monolayers 48 h after being split. Bar, 5.46 μm. (B to D) Infected monolayers. (B) Micrograph taken 24 h after infection. Bar, 2.75 μm. (C) TM4000-infected CHO monolayers 48 h after infection. Bar, 5.43 μm. (D) TM4000 grown on CHO monolayers 65 h postinfection. A microcolony of TM4000 can be seen in the upper corner of this panel. Bar, 4.08 μm.

containing plasmid pTAR46 but not by pVRC7511, which carries a *nanH* deletion (Fig. 1). We found that when VRC426 containing pTAR46 was used to infect rat granuloma pouches in single infections, the growth defect of VRC426 was completely reversed (Fig. 8B).

To prove that only the *nanH* gene of pTAR46 was responsible for the improved growth of VRC426 in the rat pouch, we also analyzed the ability of a pTAR46 derivative containing a mutated *nanH* gene to complement the growth defect. Plasmid pVRC7511 contains only the upstream region of the *nanH* gene. When VRC426 containing pVRC7511 is introduced into the rat pouch, some growth is observed 24 h postinfection (Fig. 8D). However, after 24 h, the growth rate diminished and the bacterial yield was low compared with that of VRC426 carrying a plasmid containing the intact *nanH* gene (pTAR46). It is also interesting that plasmid pVRC7511 is not retained in VRC426 cells during the limited growth observed. This is shown in Fig. 8D, in which the kinetics of growth of VRC426 containing pVRC7511 is given as the total number of bacteria determined in rich medium (growth curve b) versus the number of bacteria which retain the plasmid marker (cefoxitin resistance; growth curve f). In contrast, for VRC426/pTAR46 the total number of bacteria and the number of bacteria that retained the plasmid marker are the same (see growth curves b versus c in Fig. 8D). Both of these plasmids are derivatives of pJST61, which is unstable in the absence of selective pressure in vitro.

Finally, we carried out competition experiments with VRC426 with either the *nanH*$^+$ or *nanH*-deficient plasmid (data not shown). We found that VRC426 containing plasmid pTAR46 outgrows VRC426 with pVRC7511 in the same way that the wild-type TM4000 outgrows the mutant VRC426.

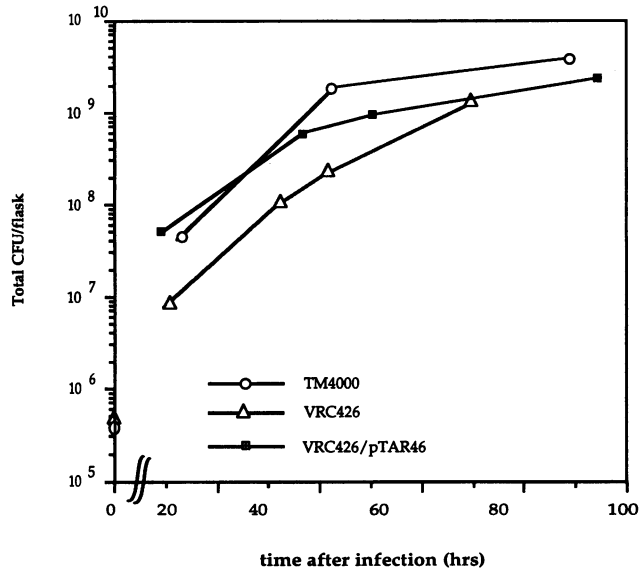


FIG. 7. Growth curve of TM4000, VRC426, and VRC426/pTAR46 on CHO monolayers. The growth curves shown in this figure are representative of at least three independent experiments with the same results for each strain shown. They are presented in the same graph only for comparison purposes. The break bar between time zero and 24 h indicates that a straight line linking these two points is not an accurate representation of the kinetics of growth during the time period (see text). The zero points were determined experimentally for each growth curve and are as follows: TM4000, $3 \times 10^5$; VRC426, $5 \times 10^5$; VRC426/pTAR46, $6 \times 10^5$.

## DISCUSSION

It has often been suggested that the presence of neuraminidase activity in a bacterial pathogen contributes to the virulence of the strains (5, 8, 9, 11, 13, 14, 16, 19). Terminal sialic acid residues, the substrates for neuraminidase action, are widely distributed on the surface of mammalian cells and seem to play an important role in maintaining the integrity of the cells and modulating the relationships between cells (10, 25, 34). Bacterial neuraminidase could profoundly disturb these interactions by removing the terminal sialic acids (25). At present, there is little specific information on the role of any bacterial neuraminidase in the establishment or maintenance of an infection.

In order to address the role of neuraminidase in *B. fragilis* pathogenesis, mutants in the *nanH* gene were used to infect two model systems. We have found that VRC404, which carries an insertion in *nanH* and is capable of reverting to *nanH*$^+$ at low frequency ($10^{-3}$ to $10^{-4}$), grows in the tissue culture monolayers and the rat granuloma pouch. However, this strain gives rise to wild-type *nanH*$^+$ derivatives at high frequency when it is grown in the model systems. By contrast, when glucose was added to the VRC404-infected monolayers throughout the active bacterial growth phase, no increase in reversion to *nanH*$^+$ was detected. Therefore, the selective pressure for the revertants in the tissue culture system seems to be the decrease in glucose concentration at later times after infection and the need of the bacteria to utilize new carbon sources for continued growth. There must also be strong selective pressure in the rat granuloma pouch because there is a rapid accumulation of *nanH*$^+$ revertants within 24 to 48 h of inoculation with VRC404. We also found that the glucose concentration fell within the rat pouch during bacterial growth. These results suggest that the *B. fragilis* neuraminidase may be playing an important nutritional role for bacterial growth in vivo.

This result is consistent with the altered growth kinetics of the *nanH* deletion strain, VRC426. When VRC426 is used to inoculate the rat granuloma pouch, a rather severe growth defect is seen. Furthermore, VRC426 displays an extreme growth disadvantage in the rat pouch when coinfected with *nanH*$^+$ wild-type cells, even when the ratio of mutant to wild-type cells is more than 10 at the time of inoculation.

What is the explanation for the ability of VRC426 to grow well in the tissue culture, while its growth is severely affected in the rat pouch? The concentration of free glucose is lower in the rat pouch than in the tissue culture system at the time of infection; thus, the rat pouch represents a more stringent growth condition than that of the tissue culture system. Therefore, *B. fragilis* cells encounter glucose starvation at earlier times in the rat pouch. The defects in VRC426 growth in the rat pouch can be completely reversed by introducing the *nanH*$^+$ plasmid pTAR46 into VRC426. In contrast, a deleted version of the *nanH* gene present in pVRC7511 does not complement the growth defect in VRC426. Moreover, in competition experiments with VRC426 carrying either pVRC7511 or pTAR46, the *nanH*$^+$ cells outgrew the strain containing the partial copy of the *nanH* gene.

Dalhoff et al. (13) reported that the $O_2$ concentration of uninfected pouches decreased with time from an initial concentration of 16.6% to 7.5%. This represents significantly aerobic conditions because 8% or higher $O_2$ levels are bacteriostatic for *B. fragilis* (22). However, Dalhoff et al. (13) found that after *E. coli* infection, the pouches become completely anaerobic within 24 h postinfection. The growth of *E. coli* under this condition is immediate and continues until an essential component is exhausted and the bacteria enter into stationary phase (13). In contrast, in the case of *B. fragilis* infection, a lag period must be required in order to establish the appropriate $pO_2$ and redox potential that will allow *Bacteroides* proliferation. The growth of wild-type *B. fragilis* cells follows this predicted pattern with an initial lag and slow growth phase followed by a faster growth phase that lasts until a plateau is reached. The *nanH* deletion strain VRC426 shows only the slow growth phase, even at late times after infection. We can postulate that the *nanH* deficiency is preventing the cells from effectively obtaining nutrients to grow. It is also possible that these cells are more sensitive to the hosts' immune defenses or even that they are impaired in their ability to create the anaerobic environment required for growth.

The results of the rat pouch competition experiments between wild-type and *nanH*-deficient strains rule out the possibility of any direct interaction of the two cell types or the elaboration of a *trans*-acting factor that might correct the defects in the mutant cells. Rather, the two cell types seem to act independently. These observations may be an indication of the way *Bacteroides* cells grow in the colon, where the supply of carbon source is variable and scarce and where there is direct competition with many other bacteria (32). We have observed that *B. fragilis* cells grow as microcolonies on the surface of the tissue culture cells and, presumably, within the rat pouch at early times after infection. These clusters may allow the bacterial cells to efficiently scavenge substrates from the complex glycoproteins and oligosaccharides present on the surface of the animal cells or the sialic acid-rich colonic mucin present in the intestinal lumen. It is interesting that most of the glycohydrolases found in *Bacteroides* spp. are cell associated (32), and thus all of the

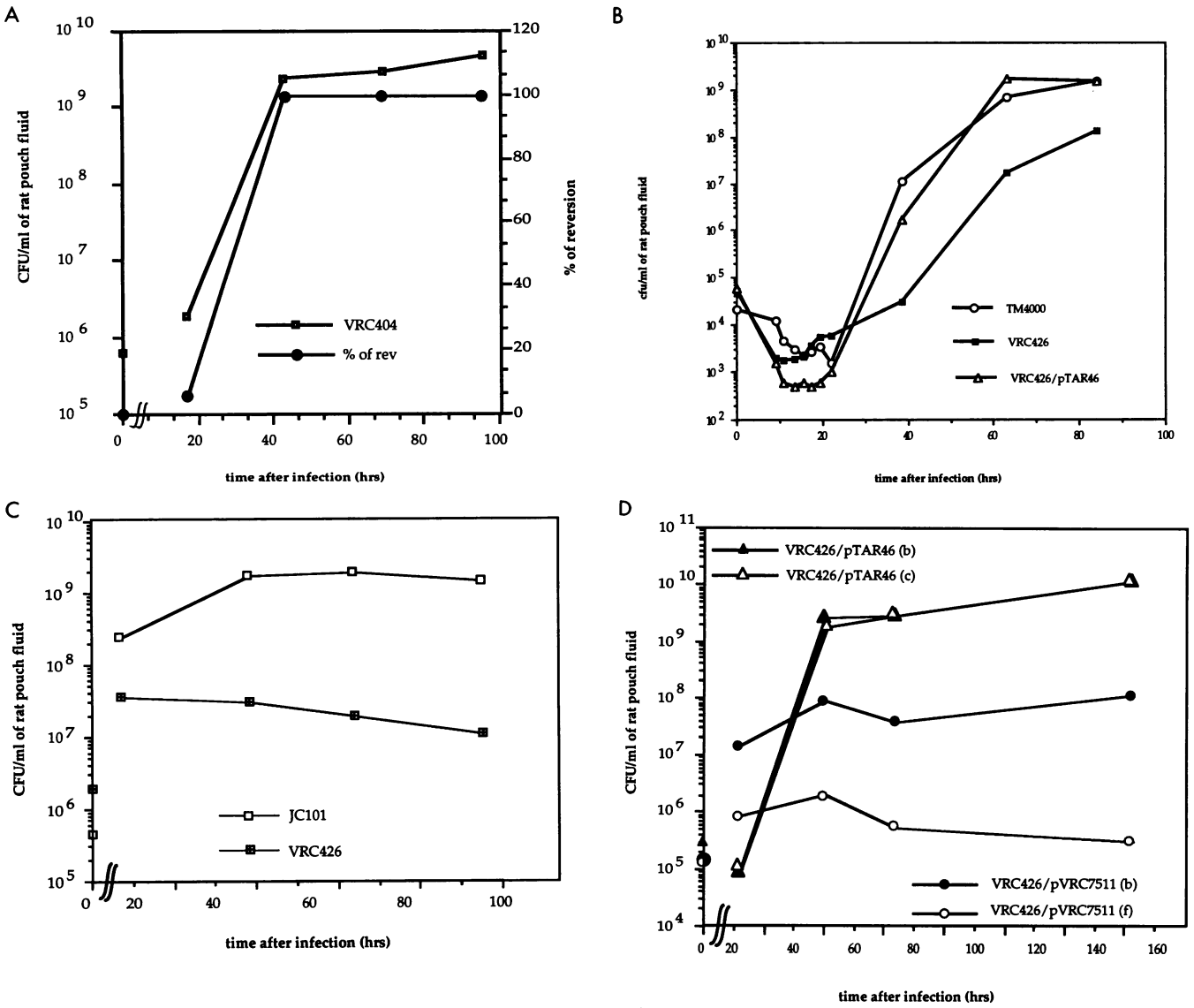


FIG. 8. Growth in the rat granuloma pouch. (A) Growth of insertion mutant VRC404 and percentage of reversion to wild-type *nanH*$^+$. This experiment is representative of four additional experiments, two of which used a lower inoculum size. In all of the experiments, all of the colonies tested had become *nanH*$^+$ by approximately 40 h after infection. (B) Growth kinetics of TM4000, VRC426, and VRC426/pTAR46. In the experiments depicted, the starting inocula were as follows: TM4000, $2 \times 10^4$, VRC426, $5.4 \times 10^4$, VRC426/pTAR46, $4.5 \times 10^4$. The inoculum size was experimentally measured in this and the repeat experiments by sampling the rat pouch immediately after inoculation. These experiments were done three times, with similar results for each strain. During the first 24 h after infection, seven samples were collected at 9, 11, 13, 15, 17, 19, and 22 h. The viable count and glucose concentration were determined for each sample. All of the strains show a similar lag time of approximately 16 h. (C) Kinetics of growth of a mixture of *nanH*$^+$(JC101) and mutant (VRC426) *B. fragilis* cells. A mixture of JC101 and VRC426 was used to infect a rat granuloma pouch at the following inocula: JC101, $4 \times 10^5$; VRC426, $2 \times 10^6$. The experiment has been repeated twice with the same inoculum size, with similar results. The bacteria were mixed prior to infection of the rat pouch. The determination of the viable counts for each strain was done by differential plating as indicated in Materials and Methods. The break lines are as in Fig. 7. (D) Growth of VRC426/pTAR46 and VRC426/pVRC7511. These experiments were with rat pouches infected independently with each strain. The solid symbols (b) indicate the viable counts of VRC426/pTAR46 and VRC426/pVRC7511 determined on BHIS plates. The open symbols (c and f) represent the viable counts of the strains determined in selective medium, c indicates BHIS supplemented with clindamycin (6 μg/ml), and f indicates BHIS supplemented with cefoxitin (25 μg/ml). The experiments shown here were repeated twice, with similar results for each strain. The zero points after infection were experimentally determined and are as follows: VRC426/pTAR46, $3 \times 10^6$; VRC426/pVRC7511, $1.5 \times 10^6$. The break lines are as in Fig. 7.

nutrients released by the action of these enzymes would remain in close association with the cluster of bacterial cells, avoiding the release of nutrients that may be used by competing bacteria.

The establishment of an infection can be divided into various phases (33), one of them being the multiplication of the microorganism in the host. In this report, we propose that, at the very least, neuraminidase activity is important for the multiplication of *B. fragilis* cells in vivo after the initial infection has taken place.

## ACKNOWLEDGMENTS

The work reported in this paper was supported by Public Health Service grant AI-19497 from the National Institutes of Health.

We thank Judith Reichler for the electron microscopy, J. Orlando and L. A. Ham (Division of Laboratory Animal Medicine of Tufts University), and A. Holmes (our laboratory) for help with the rats. We thank the Digestive Disease Center, NEMC (NIDDK, P30 DK34928), for continuous supply of tissue culture cells. We also thank C. Kumamoto, A. L. Sonenshein, M. Kessler, A. Holmes, and C. Murphy for suggestions on the manuscript and Rene Gallegos for help beyond the call of duty.

## REFERENCES

1. **Ada, G. L., and P. D. Jones.** 1986. The immune response to influenza infection. Curr. Top. Microbiol. Immunol. **128:**1–54.
2. **Arora, D. J. S., and M. Houde.** 1988. Purified glycoproteins of influenza virus stimulate cell mediated cytotoxicity *in vivo*. Nat. Immun. Cell Growth Regul. **7:**287–296.
3. **Berg, J.-O., L. Lindqvist, and C. E. Nord.** 1980. Purification of glycoside hydrolases from *Bacteroides fragilis*. Appl. Environ. Microbiol. **40:**40–47.
4. **Berg, J.-O., C.-E. Nord, and T. Wadstrom.** 1978. Formation of glycosidases in batch and continuous culture of *Bacteroides fragilis*. J. Environ. Microbiol. **35:**269–273.
5. **Berry, A. M., J. C. Paton, E. M. Glare, D. Hansman, and D. E. A. Catcheside.** 1988. Cloning and expression of the pneumococcal neuraminidase gene in *Escherichia coli*. Gene **71:**299–305.
6. **Brown, J. G., and D. C. Strauss.** 1987. Characterization of neuraminidases produced by various serotypes of group B streptococci. Infect. Immun. **55:**1–6.
7. **Claesson, B. E. B., and I. H. Gotthardsson.** 1988. A tissue culture model for study of growth promotion and antimicrobial susceptibility in *Bacteroides fragilis*. J. Antimicrob. Chemother. **21:**17–26.
8. **Colman, P. M.** 1992. Structural basis of antigenic variation: studies of influenza virus neuraminidase. Immunol. Cell Biol. **70:**209–214.
9. **Comfield, A. P., and R. Schauer.** 1982. Sialic acids. Springer-Verlag, Vienna.
10. **Cross, A. S., and D. G. Wright.** 1991. Mobilization of sialidase from intracellular stores to the surface of human neutrophils and its role in stimulated adhesion responses of these cells. J. Clin. Invest. **88:**2067–2076.
11. **Csete, M., B. I. Leu, and M. E. A. Pereira.** 1985. An influenza model for *Trypanosoma cruzi* infection: interactive roles for neuraminidase and lectin. Curr. Top. Microbiol. Immunol. **117:**153–165.
12. **Dalhoff, A., G. Frank, and G. Luckhaus.** 1982. The granuloma pouch: an *in vivo* model for pharmacokinetic and chemotherapeutic investigations. I. Biochemical and histological characterization. Infection **10:**354–360.
13. **Dalhoff, A., G. Frank, and G. Luckhaus.** 1983. The granuloma pouch: an *in vivo* model for pharmacokinetic and chemotherapeutic investigations. II. Microbial characterization. Infection **11:**49.
14. **Fearon, D. T.** 1978. Regulation by membrane sialic acid of B1H-dependent decay association of amplification C3 convertase of the alternative complement pathway. Proc. Natl. Acad. Sci. USA **75:**1971–1975.
15. **Galen, J. E., J. M. Ketley, A. Fasano, S. H. Richardson, S. S. Wasserman, and J. B. Kaper.** 1992. Role of *Vibrio cholerae* neuraminidase in the function of cholera toxin. Infect. Immun. **60:**406–415.
16. **Guzman, C. A., M. Plate, and C. Pruzzo.** 1990. Role of neuraminidase-dependent adherence in *Bacteroides fragilis* attachment to human epithelial cells. FEMS Microbiol. Lett. **59:**187–192.
17. **Hecht, D. W., and M. H. Malamy.** 1989. Tn*4399*, a conjugal mobilizing transposon of *Bacteroides fragilis*. J. Bacteriol. **171:**3603–3608.
18. **Kelly, R. T., S. Farmer, and D. Greiff.** 1967. Neuraminidase activities of clinical isolates of *Diplococcus pneumoniae*. J. Bacteriol. **94:**272–273.
19. **Maniatis, T., E. F. Fritsch, and J. Sambrook.** 1982. Molecular cloning: a laboratory manual. Cold Spring Harbor Laboratory, Cold Spring Harbor, N.Y.
20. **Moriyama, T., and L. Barksdale.** 1967. Neuraminidase of *Corynebacterium diphtheriae*. J. Bacteriol. **94:**1565–1581.
21. **Myers, R. W., R. T. Lee, Y. C. Lee, G. H. Thomas, L. W. Reynolds, and Y. Uchida.** 1980. The synthesis of 4-methylumbelliferyl α-ketoside of *N*-acetylneuraminic acid and its use in a fluorometric assay for neuraminidase. Anal. Biochem. **101:**166–174.
22. **Onderdonk, A. W., J. Johnston, J. W. Mayhew, and S. L. Gorbach.** 1976. Effect of dissolved oxygen and Eh on *Bacteroides fragilis* during continuous culture. Appl. Environ. Microbiol. **31:**168–172.
23. **Palese, P., K. Tobita, M. Ueda, and R. W. Compans.** 1974. Characterization of temperature-sensitive influenza virus mutants defective in neuraminidase. Virology **61:**397–410.
24. **Patrick, S.** 1993. Virulence of *Bacteroides fragilis*. Rev. Med. Microbiol. **4:**40–49.
25. **Pilatte, Y., J. Bignon, and C. R. Lambré.** 1993. Sialic acids as important molecules in the regulation of the immune system: pathophysiological implications of sialidases in immunity. Glycobiology **3:**201–217.
26. **Postek, M. T., K. S. Howard, A. H. Johnson, and K. L. McMichael.** 1980. Scanning electron microscopy. A student's handbook. Ladd Research Industries, Inc., Burlington, Vt.
27. **Reed, K. C., and D. A. Mann.** 1985. Rapid transfer of DNA from agarose gels to nylon membranes. Nucleic Acids Res. **13:**7207–7221.
28. **Robillard, N. J., F. P. Tally, and M. H. Malamy.** 1985. Tn*4400*, a compound transposon isolated from *Bacteroides fragilis*, functions in *Escherichia coli*. J. Bacteriol. **164:**1248–1255.
29. **Rosen, S. D., S. I. Chi, D. D. True, M. S. Singer, and T. A. Yednock.** 1989. Intravenously injected sialidase inactivates attachment sites for lymphocytes on high endothelial venules. J. Immunol. **142:**1895–1902.
30. **Rothe, B., B. Rothe, P. Roggentin, and R. Schauer.** 1991. The sialidase gene from *Clostridium septicum*: cloning, sequencing, expression in *Escherichia coli* and identification of conserved sequences. Mol. Gen. Genet. **226:**190–197.
31. **Russo, T. A., J. S. Thompson, V. G. Godoy, and M. H. Malamy.** 1990. Cloning and expression of the *Bacteroides fragilis* TAL2480 neuraminidase gene, *nanH*, in *Escherichia coli*. J. Bacteriol. **172:**2594–2600.
32. **Salyers, A. A.** 1979. Energy sources of major intestinal fermentative anaerobes. Am. J. Clin. Nutr. **32:**158–163.
33. **Schaechter, M., G. Medoff, and D. Schlessinger.** 1989. Mechanisms of microbial disease. Williams & Wilkins, Baltimore.
34. **Schauer, R.** 1985. Sialic acids and their role as biological masks. Trends Biochem. Sci. **10:**357–360.
35. **Southern, E. M.** 1975. Detection of specific sequences among DNA fragments separated by gel electrophoresis. J. Mol. Biol. **98:**503–517.
36. **Tamura, M., R. G. Webster, and F. A. Ennis.** 1991. Antibodies to HA and NA augment uptake of influenza A viruses into cells via Fc receptor entry. Virology **182:**211–219.
37. **Tanaka, H., F. Ito, and T. Iwasaki.** 1992. Purification and characterization of a sialidase from *Bacteroides fragilis* SBT3182. Biochem. Biophys. Res. Commun. **189:**524–529.
38. **Thompson, J. S., and M. H. Malamy.** 1990. Sequencing the gene for an imipenem-cefoxitin-hydrolyzing enzyme (*cfiA*) from *Bacteroides fragilis* TAL2480 reveals strong similarity between CfiA and *Bacillus cereus* β-lactamase II. J. Bacteriol. **172:**2584–2593.
39. **Vimr, E. R., L. Lawrisuk, J. Galen, and J. B. Kaper.** 1988. Cloning and expression of the *Vibrio cholerae* neuraminidase gene *nanH* in *Escherichia coli*. J. Bacteriol. **170:**1495–1504.